Feasible Path Identification in Optimal Power Flow with Sequential Convex Restriction

Dongchan Lee, Konstantin Turitsyn, Daniel K. Molzahn, and Line A. Roald

***Abstract*—Nonconvexity induced by the nonlinear AC power flow equations challenges solution algorithms for AC optimal power flow (OPF) problems. While significant research efforts have focused on reliably computing high-quality OPF solutions, identifying a feasible path from an initial operating to a desired operating point is a topic that has received much less attention. However, since the feasible space of the OPF problem is nonconvex and potentially disconnected, it can be challenging to transition between operating points while avoiding constraint violations. To address this problem, we propose an algorithm which computes a provably feasible path from an initial operating point to a desired operating point. The algorithm solves a sequence of quadratic optimization problems over conservative convex inner approximations of the OPF feasible space, each representing a so-called convex restriction. In each iteration, we obtain a new, improved operating point and a feasible transition from the operating point in the previous iteration. In addition to computing a feasible path to a known desired operating point, this algorithm can also be used to locally improve the operating point. Extensive numerical studies on a variety of test cases demonstrate the algorithm and the ability to arrive at a high-quality solution in few iterations.**

I. Introduction

AC optimal power flow (OPF) is a fundamental optimization problem in power system analysis [1]. The classical form of an OPF problem [2] seeks an operating point that is *feasible* (i.e., satisfies both the AC power flow equations that model the network physics and the inequality constraints associated with operational limits on voltage magnitudes, line flows, generator outputs, etc.) and economically efficient (i.e., achieves *minimum operational cost*). Significant research efforts have focused on obtaining locally and globally optimal OPF solutions using algorithms based on local search, approximation, and relaxation techniques [3]–[6]. While previous research has improved the computational tractability of OPF algorithms and the quality of the resulting solutions, a number of challenging issues remain. One such issue is to determine a *sequence* of control actions that facilitate a safe transition from the current operating point to the desired operating point [1], [7].

Previous literature has considered the problem of determining a *limited number* of active and reactive power redispatch [8]–[10] required to bring the system to a new safe or optimal operating point. References such as [9], [10] consider the sequence as a set of individual control actions, where the operating point after each action must be steady-state feasible. While this improves security relative to a setting where intermediate feasibility is not considered, the feasible space of the AC OPF problem is nonconvex and sometimes disconnected [11]. Hence, a *feasible path* connecting the two steady-state operating points (where each intermediate state is feasible) can be difficult to compute or may not exist. Despite the importance of maintaining system security, there is only limited previous work on the topic of ensuring feasibility on the path from the current to a desired operating point. Recent approaches in [12] and [13] guarantee power flow feasibility for sets of power injections, but are only applicable to distribution systems. The work in [13] ensures that the system's trajectory remains feasible, but is limited to systems with only PQ buses and the nonconvexity of the associated condition precludes the use of scalable convex optimization solvers. Approaches for robust AC OPF problems, such as [14]–[16], have also considered feasibility for ranges of power injections, but rely on convex relaxation of the AC power flow [14], require controllable power injections on every node [15], or only guarantee feasibility of inequality constraints [16].

To the best of our knowledge, this paper proposes the first algorithm that provides a guaranteed feasible path for a general OPF problem. Specifically, we propose an algorithm for computing a sequence of control actions that ensures feasibility with respect to both the nonlinear AC power flow equations and operational limits (in the form of inequality constraints) as the system transitions from one operating point to another. In contrast to previous work, our proposed feasible path algorithm is not limited to specific classes of systems, considers the nonlinear AC power flow model, and is tractable for large problems. Based on a quadratic convex restriction of the AC power flow feasible space [17], we compute a piece-wise linear path connecting an initial point to a desired operating point such that all points along the path are feasible. The proposed algorithm is illustrated in Fig. 1.

We highlight two characteristics of the convex restriction

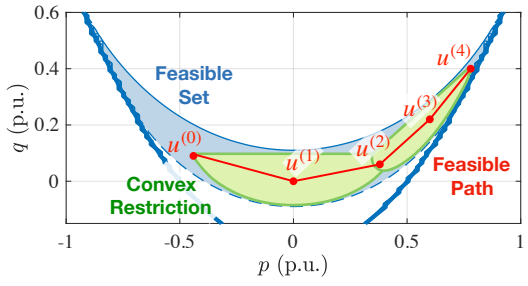

Fig. 1. Illustration of a feasible path identification for a two-bus system. The region in blue is the nonconvex feasible space. To find a feasible path from the initial operating point $u^{(0)}$ to the desired operating point $u^{(4)}$, our algorithm constructs a sequence of convex restrictions (shown in green). By iteratively solving optimization problems over the convex restrictions, we obtain a sequence of intermediate points that together form a feasible, piece-wise linear path $u^{(0)}$–$u^{(1)}$–$u^{(2)}$–$u^{(3)}$–$u^{(4)}$.

which are crucial for the success of our algorithm:
(i) The convex restriction provides a *conservative inner approximation* of the feasible space of the AC power flow equations, which implies that all points within the restriction are AC power flow feasible (and, by proper extensions, feasible for additional inequality constraints). This is in contrast to convex relaxations, which extend the originally nonconvex feasible space to become convex by adding infeasible points.
(ii) The convex restriction is, as the name implies, a convex set. This means that the transition between any two points within the convex restriction will also lie inside the convex restriction, hence guaranteeing that there exists a feasible AC power flow solution at any intermediate point.

In summary, the main contributions of this paper are:

1. We formulate the AC OPF problem based on convex restrictions from [17]. This is the first formulation of an OPF with convex restriction, which requires extending the convex restriction to include line flow constraints. The formulation guarantees that the linear trajectory between any two points within the restriction is feasible, is applicable to general system models, considers the nonlinear AC power flow equations, and is tractable for large problems.
2. Using the OPF with convex restriction, we propose a sequential algorithm which in each iteration (i) constructs a convex restriction around a feasible point and (ii) solves the OPF problem to obtain an improved feasible point. The algorithm outcome is a piece-wise linear, feasible path. We provide two objective functions which either achieve local improvements to the current operating point or identify a feasible path to a desired operating point.
3. We demonstrate the capabilities of the algorithm using numerical experiments on a variety of test cases.

The rest of the paper is organized as follows. Section II presents the system model and preliminaries. Section III reviews and extends convex restriction techniques to formulate the OPF problem including line flow limits and other features. Section IV presents our algorithm for computing OPF solutions with corresponding feasible paths. Section V demonstrates the proposed algorithm with numerical experiments and illustrative figures. Section VI concludes the paper.

II. System Model and Preliminaries

Consider a power network with sets of buses $\mathcal{N}$ and lines $\mathcal{E} \subseteq \mathcal{N}\times\mathcal{N}$. The scalars n_b, n_g, n_{pq}, and n_l denote the number of buses, generators, PQ buses, and lines. The network's incidence matrix is $E \in \mathbb{R}^{n_b\times n_l}$. The connection matrix between generators and buses is $C \in \mathbb{R}^{n_b\times n_g}$, where the (i,k) element of C is equal to 1 for each bus i and generator k and zero otherwise. The active and reactive power generations are $p_{\mathrm{g}} \in \mathbb{R}^{n_g}$ and $q_{\mathrm{g}} \in \mathbb{R}^{n_g}$. Specified values of active and reactive load demands are denoted $p_{\mathrm{d}} \in \mathbb{R}^{n_b}$ and $q_{\mathrm{d}} \in \mathbb{R}^{n_b}$. The buses' voltage magnitudes and phase angles are $v \in \mathbb{R}^{n_b}$ and $\theta \in \mathbb{R}^{n_b}$. The superscripts "f" and "t" denote *from* and *to* buses for the lines. The subscripts "vθ", "ns", "pv", and "pq" denote the slack (vθ), non-slack (non-vθ), PV, and PQ elements of the corresponding vector. Superscript "T" denotes the transpose. I and $\mathbf{0}$ denotes identity and zero matrix of appropriate size.

A. Phase-Adjusted AC Power Flow Formulation

To set the stage for our further discussion, we describe a slightly modified representation of the standard AC power flow equations, the so-called *phase-adjusted AC power flow formulation*. The formulation is defined relative to a known, feasible *base point* denoted by the subscript 0, i.e., v_0 and θ_0 denote the base point's voltage magnitude and phase angle.

The angle differences across each line are

$$\varphi_l = \theta_l^{\mathrm{f}} - \theta_l^{\mathrm{t}}, \qquad l = 1,\dots,n_l, \tag{1}$$

where θ_l^{f} and θ_l^{t} denote the phase angle of the *from* bus and *to* bus of line l. This can be equivalently expressed as $\varphi = E^T\theta$. The *phase-adjusted* angle differences are then defined as

$$\tilde{\varphi} = \varphi - \varphi_0 = E^T\theta - E^T\theta_0 = E^T(\theta - \theta_0).$$

With this, the phase-adjusted directed AC Power Flow equations can be written for each bus $k = 1,\dots,n_b$,

$$p_k^{\mathrm{inj}} = \sum_{l=1}^{n_l} v_l^{\mathrm{f}} v_l^{\mathrm{t}} \left(\widehat{G}_{kl}^{c}\cos\tilde{\varphi}_l + \widehat{B}_{kl}^{s}\sin\tilde{\varphi}_l\right) + G_{kk}^{d} v_k^2, \tag{2a}$$

$$q_k^{\mathrm{inj}} = \sum_{l=1}^{n_l} v_l^{\mathrm{f}} v_l^{\mathrm{t}} \left(\widehat{G}_{kl}^{s}\sin\tilde{\varphi}_l - \widehat{B}_{kl}^{c}\cos\tilde{\varphi}_l\right) - B_{kk}^{d} v_k^2, \tag{2b}$$

where v_l^{f} and v_l^{t} denote the voltage magnitude at the *from* and *to* buses of line l. The active and reactive power injections are $p^{\mathrm{inj}} = Cp_{\mathrm{g}} - p_{\mathrm{d}}$ and $q^{\mathrm{inj}} = Cq_{\mathrm{g}} - q_{\mathrm{d}}$. The matrices $\widehat{G}^{\mathrm{c}}$, $\widehat{G}^{\mathrm{s}}$, $\widehat{B}^{\mathrm{c}}$, $\widehat{B}^{\mathrm{s}} \in \mathbb{R}^{n_b\times n_l}$ and G^d, $B^d \in \mathbb{R}^{n_b\times n_b}$ are phase-adjusted admittance matrices defined relative to the base point, and their derivations are shown in the Appendix. In addition to the power flow equations in (2), the OPF problem enforces the following operational constraints:

$$p_{\mathrm{g},i}^{\min} \le p_{\mathrm{g},i} \le p_{\mathrm{g},i}^{\max},\ q_{\mathrm{g},i}^{\min} \le q_{\mathrm{g},i} \le q_{\mathrm{g},i}^{\max}, \qquad i=1,\dots,n_g, \tag{3a}$$

$$v_j^{\min} \le v_j \le v_j^{\max}, \qquad j=1,\dots,n_b \tag{3b}$$

$$\varphi_l^{\min} \le \varphi_l \le \varphi_l^{\max}, \qquad l=1,\dots,n_l, \tag{3c}$$

$$(s_{p,l}^{\mathrm{f}})^2 + (s_{q,l}^{\mathrm{f}})^2 \le (s_l^{\max})^2, \qquad l=1,\dots,n_l, \tag{3d}$$

$$(s_{p,l}^{\mathrm{t}})^2 + (s_{q,l}^{\mathrm{t}})^2 \le (s_l^{\max})^2, \qquad l=1,\dots,n_l. \tag{3e}$$

Here, (3a) represents the generators' active and reactive power capacity limits, $p_g^{\max}, p_g^{\min}$ and $q_g^{\max}, q_g^{\min}$, respectively. Eqs. (3b), (3c) limit the voltage magnitudes to the range $v^{\min}, v^{\max}$ and enforce stability limits on the angle differences $\varphi^{\min}, \varphi^{\max}$. Eqs. (3d), (3e) impose the line capacity limit $s^{\max}$ where $s_{p,l}^{\mathrm{f}}$, $s_{q,l}^{\mathrm{f}}$ represent the active and reactive power flowing into the line l at the *from* buses, and $s_{p,l}^{\mathrm{t}}$, $s_{q,l}^{\mathrm{t}}$ represent the active and reactive power flowing into the line l at the *to* buses.

The phase-adjusted AC power flow equations can be expressed in terms of basis functions, which are defined as

$$\begin{aligned}
\psi_l^{\mathrm{C}}(v,\varphi) &= v_l^{\mathrm{f}} v_l^{\mathrm{t}} \cos(\varphi_l - \varphi_{0,l}), && l = 1,\dots,n_l,\\
\psi_l^{\mathrm{S}}(v,\varphi) &= v_l^{\mathrm{f}} v_l^{\mathrm{t}} \sin(\varphi_l - \varphi_{0,l}), && l = 1,\dots,n_l,\\
\psi_k^{\mathrm{Q}}(v,\varphi) &= v_k^2, && k = 1,\dots,n_b.
\end{aligned} \tag{4}$$

The power flow equations (2) can then be rewritten as

$$\begin{bmatrix} Cp_{\mathrm{g}} - p_{\mathrm{d}} \\ Cq_{\mathrm{g}} - q_{\mathrm{d}} \end{bmatrix} + \begin{bmatrix} -\widehat{G}^{\mathrm{c}} & -\widehat{B}^{\mathrm{s}} & -G^{\mathrm{d}} \\ \widehat{B}^{\mathrm{c}} & -\widehat{G}^{\mathrm{s}} & B^{\mathrm{d}} \end{bmatrix} \psi(v,\varphi) = 0, \tag{5}$$

where $\psi(v,\varphi) = \begin{bmatrix}\psi^{\mathrm{C}}(v,\varphi)^T & \psi^{\mathrm{S}}(v,\varphi)^T & \psi^{\mathrm{Q}}(v,\varphi)^T\end{bmatrix}^T$.

B. Control and State Variables

Standard power system definitions divide the system into three sets of buses:

- PV buses: $p_{\text{pv}}^{\text{inj}}$, v_{pv} specified; $q_{\text{pv}}^{\text{inj}}$, θ_{pv} implicitly defined.
- PQ buses: $p_{\text{pq}}^{\text{inj}}$, $q_{\text{pq}}^{\text{inj}}$ specified; v_{pq}, θ_{pq} implicitly defined.
- Vθ (slack) bus: $v_{\text{v}\theta}$, $\theta_{\text{v}\theta}$ specified; $p_{\text{v}\theta}^{\text{inj}}$, $q_{\text{v}\theta}^{\text{inj}}$ implicitly defined.

For the analysis, variables that are explicitly set by the system operator are control variables, and variables that are implicitly determined through the AC power flow equations are state variables. Constants such as the active and reactive power load on PQ buses and the reference angle $\theta_{\text{v}\theta}=0$ are not considered as variables. The *control* variables are the active power outputs of generators at PV buses p_{pv} and the voltage magnitudes at the Vθ and PV buses v_{g}, denoted by $u=[p_{\text{pv}}, v_{\text{g}}] \in \mathbb{R}^{2n_g-1}$. For the sake of clarity, we differentiate between the *state* variables $x = [\theta_{ns}, v_{pq}] \in \mathbb{R}^{n_b-1+n_{pq}}$ which are implicitly defined through the power flow equations given a set of control variables u, and the *intermediate* variables $[p_{\text{v}\theta}, q_{\text{v}\theta}, q_{\text{pv}}]$ which are explicitly defined by the power flow equations and a given set of state and control variables (x, u).

For a given set of control variables u, the state variables x can be obtained from a subset of the phase-adjusted power flow equations (5),

$$\underbrace{\begin{bmatrix} C_{\text{ns}} p_{\text{g}} - p_{\text{d,ns}} \\ C_{\text{pq}} q_{\text{g}} - q_{\text{d,pq}} \end{bmatrix}}_{\tau(u)} + \underbrace{\begin{bmatrix} -\widehat{G}^{\text{c}}_{\text{ns}} & -\widehat{B}^{\text{s}}_{\text{ns}} & -G^{\text{d}}_{\text{ns}} \\ \widehat{B}^{\text{c}}_{\text{pq}} & -\widehat{G}^{\text{s}}_{\text{pq}} & B^{\text{d}}_{\text{pq}} \end{bmatrix}}_{M_{\text{eq}}} \psi(v,\varphi) = 0, \quad (6)$$

where $\tau(u)$ denotes the active and reactive power injections at certain buses. The matrix $\widehat{G}^{\text{c}}_{\text{ns}} \in \mathbb{R}^{(n_b-1)\times n_l}$ contains the rows corresponding to the non-slack buses from $\widehat{G}^{\text{c}} \in \mathbb{R}^{n_b \times n_l}$, and $\widehat{B}^{\text{c}}_{\text{pq}} \in \mathbb{R}^{n_{pq}\times n_l}$ contains the rows corresponding to PQ buses from $\widehat{B}^{\text{c}} \in \mathbb{R}^{n_b \times n_l}$. The other submatrices are defined similarly. Note that (6) is a square system of equations.

The intermediate variables (i.e., the active power at the Vθ bus $p_{\text{v}\theta}$ and the reactive power at the Vθ and PV buses $q_{\text{v}\theta}, q_{\text{pv}}$) are functions of state and control variables (x, u):

$$\underbrace{\begin{bmatrix} C_{\text{v}\theta} p_{\text{g}} - p_{\text{d,v}\theta} \\ C_{\text{v}\theta} q_{\text{g}} - q_{\text{d,v}\theta} \\ C_{\text{pv}} q_{\text{g}} - q_{\text{d,pv}} \end{bmatrix}}_{\zeta(p_g, q_g)} = \underbrace{\begin{bmatrix} \widehat{G}^{\text{c}}_{\text{v}\theta} & \widehat{B}^{\text{s}}_{\text{v}\theta} & G^{\text{d}}_{\text{v}\theta} \\ -\widehat{B}^{\text{c}}_{\text{v}\theta} & \widehat{G}^{\text{s}}_{\text{v}\theta} & -B^{\text{d}}_{\text{v}\theta} \\ -\widehat{B}^{\text{c}}_{\text{pv}} & \widehat{G}^{\text{s}}_{\text{pv}} & -B^{\text{d}}_{\text{pv}} \end{bmatrix}}_{M_{\text{ineq}}} \psi(v,\varphi). \quad (7)$$

Line flows can be represented in terms of the phase adjusted basis functions,

$$\underbrace{\begin{bmatrix} s^{\text{f}}_p \\ s^{\text{f}}_q \end{bmatrix}}_{s^{\text{f}}} = \underbrace{\begin{bmatrix} G_{\text{ft}} & B_{\text{ft}} & G_{\text{ff}} E_{\text{f}}^T \\ -B_{\text{ft}} & G_{\text{ft}} & -B_{\text{ff}} E_{\text{f}}^T \end{bmatrix}}_{L^{\text{f}}_{\text{line}}} \psi(v,\varphi), \quad (8)$$

$$\underbrace{\begin{bmatrix} s^{\text{t}}_p \\ s^{\text{t}}_q \end{bmatrix}}_{s^{\text{t}}} = \underbrace{\begin{bmatrix} G_{\text{tf}} & -B_{\text{tf}} & G_{\text{tt}} E_{\text{t}}^T \\ -B_{\text{tf}} & -G_{\text{tf}} & -B_{\text{tt}} E_{\text{t}}^T \end{bmatrix}}_{L^{\text{t}}_{\text{line}}} \psi(v,\varphi), \quad (9)$$

where the block matrices in $L^{\text{f}}_{\text{line}}$ and $L^{\text{t}}_{\text{line}}$ are provided in the Appendix.

C. Phase-Adjusted AC Optimal Power Flow

The AC OPF problem can be written based on the phase-adjusted AC power flow with the consideration of state and control variables. This formulation is equivalent to the classical form of the AC OPF problem without any approximation. The AC OPF problem identifies the operating point with minimum generation cost while respecting the operational constraints:

$$\underset{x,u,\overline{s}^{\text{f}},\overline{s}^{\text{t}}}{\text{minimize}} \quad c(p_{\text{g}}) = \sum_{i=1}^{n_g} c_i(p_{\text{g},i}) \quad (10a)$$

$$\text{subject to} \quad \tau(u) + M_{\text{eq}}\psi(v,\varphi) = 0 \quad (10b)$$

$$\zeta(p_g^{\min}, q_g^{\min}) \le M_{\text{ineq}}\psi(v,\varphi) \le \zeta(p_g^{\max}, q_g^{\max}) \quad (10c)$$

$$\underbrace{\begin{bmatrix} E_{\text{ns}}^T & \mathbf{0} \\ \mathbf{0} & I \\ -E_{\text{ns}}^T & \mathbf{0} \\ \mathbf{0} & -I \end{bmatrix}}_{A} x \le \underbrace{\begin{bmatrix} \varphi^{\max} \\ v_{\text{pq}}^{\max} \\ -\varphi^{\min} \\ -v_{\text{pq}}^{\min} \end{bmatrix}}_{b^{\max}}, \quad \underbrace{\begin{bmatrix} p_{\text{pv}}^{\min} \\ v_{\text{g}}^{\min} \end{bmatrix}}_{u^{\min}} \le u \le \underbrace{\begin{bmatrix} p_{\text{pv}}^{\max} \\ v_{\text{g}}^{\max} \end{bmatrix}}_{u^{\max}} \quad (10d)$$

$$\begin{aligned} &|L^{\text{f}}_{\text{line}}\psi(x,u)| \le \overline{s}^{\text{f}}, \ |L^{\text{t}}_{\text{line}}\psi(x,u)| \le \overline{s}^{\text{t}} \\ &\left(\overline{s}^{\text{f}}_p\right)^2 + \left(\overline{s}^{\text{f}}_q\right)^2 \le \left(s^{\max}\right)^2, \ \left(\overline{s}^{\text{t}}_p\right)^2 + \left(\overline{s}^{\text{t}}_q\right)^2 \le \left(s^{\max}\right)^2 \end{aligned} \quad (10e)$$

The cost function of each generator i, $c_i(p_{g,i})$, is assumed to be monotonically increasing with respect to the active power generation. Eq. (10b) contains the subset of power flow equations which relate the control and state variables. Eq. (10c) imposes constraints on the intermediate variables (the active power on the Vθ bus and reactive power on generator buses). The matrix $E_{\text{ns}} \in \mathbb{R}^{(n_b-1)\times n_l}$ is a submatrix of E that selects the rows corresponding to the non-slack buses.

III. Optimal Power Flow with Convex Restriction

In this section, we summarize the procedure of obtaining a *convex restriction* for the AC OPF problem. A convex restriction provides a convex condition on the control variables u such that there exists state variables x that satisfy both the AC power flow equations in (2) and the operational constraints in (3). A sufficient convex condition for AC power flow feasibility was developed in [17], and we extend its application to solve the full OPF problem including line flow limits.

A. Quadratic Convex Restriction of Feasible Region

1) Power flow constraints in fixed point form: The convex restriction is constructed around the known, feasible base point (x_0, u_0), which is assumed to have a non-singular power flow Jacobian[1] with respect to the state variables. Consider the power flow equation (6) as finding the zeros of $f(x,u) = \tau(u) + M_{\text{eq}}\psi(v,\varphi)$. Let us denote the Jacobian with respect to x as $J_{f,0} = \nabla_x f|_{(x_0,u_0)} = M_{\text{eq}} J_{\psi,0}$ where $J_{\psi,0} = \nabla_x \psi(v, E^T\theta)|_{(v_0,\varphi_0)}$. Then, we can write the power flow equations in the following fixed-point form

$$\begin{aligned} x &= -J_{f,0}^{-1}(f(x,u) - J_{f,0}x) \\ &= -J_{f,0}^{-1}\left(M_{eq}g(x,u) + \tau(u)\right), \end{aligned} \quad (11)$$

[1]If the power flow Jacobian is singular, the system is operating at the nose of PV curve where the solution to power flow equation can disappear by an arbitrary small perturbation in the power injection.

where $g(x,u)$ represents the residual of the basis functions,

$$g(x,u) = \psi(v,\varphi) - J_{\psi,0}x. \tag{12}$$

Note that (11) corresponds to a single iteration of the Newton-Raphson procedure, which is commonly used to solve the power flow equations.

2) Sufficient condition for existence of x: The derivation of the sufficient condition for AC power flow solvability relies on Brouwer Fixed Point Theorem.

Theorem 1. (Brouwer Fixed Point Theorem [18]) Let $\mathcal{P} \subseteq \mathbb{R}^n$ be a nonempty compact convex set and $F : \mathcal{P} \to \mathcal{P}$ be a continuous mapping. Then there exists some $x \in \mathcal{P}$ such that $F(x) = x$.

In our approach, the map F corresponds to the power flow equations (11). We define the self-mapping set $\mathcal{P}$ as

$$\begin{aligned}\mathcal{P}(b) &= \{x \mid \underline{\varphi} \le \varphi \le \overline{\varphi},\ \underline{v}_{\text{pq}} \le v_{\text{pq}} \le \overline{v}_{\text{pq}}\} \\ &= \{x \mid Ax \le b\},\end{aligned} \tag{13}$$

where the matrix A is defined in (10d) and the bound b is

$$b = \begin{bmatrix}\overline{\varphi}^T & \overline{v}_{\text{pq}}^T & -\underline{\varphi}^T & -\underline{v}_{\text{pq}}^T\end{bmatrix}^T. \tag{14}$$

The polytope $\mathcal{P}(b)$ is a closed and compact set parametrized by the bounds b, which provides the upper and lower bound on the state variables. These bounds b are *not* the same as the limits provided in (3c), but are decision variables. Then Brouwer fixed point condition is equivalent to existence of $b \in \mathbb{R}^{(2n_{pq}+2n_l)}$ such that

$$\max_{x\in\mathcal{P}(b)} Kg(x,u) - AJ_{f,0}^{-1}\tau(u) \le b, \tag{15}$$

where $K = -AJ_{f,0}^{-1}M_{eq}$.

3) Concave envelopes and bounds for $g(x,u)$ and $\psi(x,u)$: A *concave envelope* of a function $g(x,u)$ is given by a concave under-estimator $\underline{g}_k(x,u)$ and a convex over-estimator $\overline{g}_k(x,u)$, such that

$$\underline{g}_k(x,u) \le g_k(x,u) \le \overline{g}_k(x,u). \tag{16}$$

Given this concave envelope, the bound on g_k over the domain $\mathcal{P}(b)$ is

$$\begin{aligned}\overline{g}_{\mathcal{P},k}(u,b) &\ge \max_{x\in\mathcal{P}(b)} \overline{g}_k(x,u) = \max_{x\in\partial\mathcal{P}_k(b)} \overline{g}_k(x,u), \\ \underline{g}_{\mathcal{P},k}(u,b) &\le \min_{x\in\mathcal{P}(b)} \underline{g}_k(x,u) = \min_{x\in\partial\mathcal{P}_k(b)} \underline{g}_k(x,u),\end{aligned} \tag{17}$$

where $\partial\mathcal{P}_k(b)$ is the set of vertices in polytope $\mathcal{P}(b)$ that are involved in function $g_k(x,u)$. For the second equality, we exploit the fact that since the envelopes are concave for the minimization problem and convex for the maximization problem in (17), the extreme values $\overline{g}_{\mathcal{P},k}(u,b), \underline{g}_{\mathcal{P},k}(u,b)$ will occur at one of the vertices in $\partial\mathcal{P}(b)$. Hence, we can ensure max/min inequality hold over the polytope by requiring all vertices to satisfy the above inequalities. Fig. 2 illustrates the concave envelope and the bounds over the polytope $\mathcal{P}(b)$ for an example function.

In the power flow equations, the functions $g(x,u)$ can be expressed as a combination of bilinear, cosine, and sine functions. The concave envelopes for these functions from [17] are provided below. The envelopes of a bilinear function are

$$\begin{aligned}\langle xy\rangle^Q &\ge -\frac{1}{4}[(x-x_0)-(y-y_0)]^2 + x_0y + xy_0 - x_0y_0, \\ \langle xy\rangle^Q &\le \frac{1}{4}[(x-x_0)+(y-y_0)]^2 + x_0y + xy_0 - x_0y_0.\end{aligned}$$

For trigonometric functions, we exploit the angle difference limits with the phase-adjusted power flow formulation to construct a tight concave envelope. Assuming $\varphi^{\max} \in [0,\ \pi]$ and $\varphi^{\min} \in [-\pi,\ 0]$, the concave envelopes for the sine and cosine functions are

$$\begin{aligned}\langle \sin\tilde{\varphi}\rangle^S &\ge \tilde{\varphi} + \left(\frac{\sin\tilde{\varphi}^{\max} - \tilde{\varphi}^{\max}}{(\tilde{\varphi}^{\max})^2}\right)\tilde{\varphi}^2,\ \ \tilde{\varphi} < \tilde{\varphi}^{\max}, \\ \langle \sin\tilde{\varphi}\rangle^S &\le \tilde{\varphi} + \left(\frac{\sin\tilde{\varphi}^{\min} - \tilde{\varphi}^{\min}}{(\tilde{\varphi}^{\min})^2}\right)\tilde{\varphi}^2,\ \ \tilde{\varphi} > \tilde{\varphi}^{\min}, \\ \langle \cos\tilde{\varphi}\rangle^C &\ge 1 - \frac{1}{2}\tilde{\varphi}^2,\quad \langle \cos\tilde{\varphi}\rangle^C \le 1.\end{aligned}$$

The upper bounds on $g(x,u)$ over $\mathcal{P}(b)$ are defined as

$$\begin{aligned}\overline{g}^C_{\mathcal{P},l}(u,b) &\ge \max_{x_l\in\mathcal{X}_l} \langle\langle v_l^{\text{f}} v_l^{\text{t}}\rangle^Q \langle\cos\tilde{\varphi}_l\rangle^C\rangle^Q - v_{0,l}^{\text{f}} v_l^{\text{t}} - v_l^{\text{f}} v_{0,l}^{\text{t}}, \\ \overline{g}^{\text{S}}_{\mathcal{P},l}(u,b) &\ge \max_{x_l\in\mathcal{X}_l} \langle\langle v_l^{\text{f}} v_l^{\text{t}}\rangle^Q \langle\sin\tilde{\varphi}_l\rangle^S\rangle^Q - v_{0,l}^{\text{f}} v_{0,l}^{\text{t}}\tilde{\varphi}_l, \\ \overline{g}^Q_{\mathcal{P},k}(u,b) &\ge \max_{v_k\in\{\overline{v}_k,\underline{v}_k\}} \langle v_k v_k\rangle^Q - 2v_k,\end{aligned}$$

where $x_l = (v_l^{\text{f}},\ v_l^{\text{t}},\ \tilde{\varphi}_l)$ and $\mathcal{X}_l = \{(v_l^{\text{f}}, v_l^{\text{t}}, \tilde{\varphi}_l) \mid v_l^{\text{f}} \in \{\underline{v}_l^{\text{f}},\ \overline{v}_l^{\text{f}}\},\ v_l^{\text{t}} \in \{\underline{v}_l^{\text{t}},\ \overline{v}_l^{\text{t}}\},\ \tilde{\varphi}_l \in \{\underline{\varphi}_k - \varphi_{0,k},\ \overline{\varphi}_k - \varphi_{0,k}\}\}$. Note that the number of vertices that need to be checked for each line is constant, i.e., the cardinality of $\mathcal{X}_l$ is 2^3 regardless of the size of the system. Similarly, $\underline{g}_{\mathcal{P},k}(u,b)$ are defined by replacing maximization with minimization and changing the direction of inequality sign, and $\overline{\psi}_{\mathcal{P},k}(u,b)$ and $\underline{\psi}_{\mathcal{P},k}(u,b)$ are defined by replacing the function g by ψ.

4) Convex restriction of OPF feasible region: The above upper and lower bounds on $g(x,u)$ over the region $\mathcal{P}(b)$ allow us to guarantee that condition (15) for power flow feasibility holds. Similarly, the bounds on $\psi(x,u)$ are used to ensure satisfaction of the inequality constraints (10c)–(10e). The resulting convex restriction represents a convex inner approximation of the feasible region in the OPF problem. This is proven by the following Theorem from [17], which we extend to include transmission line flow limits.

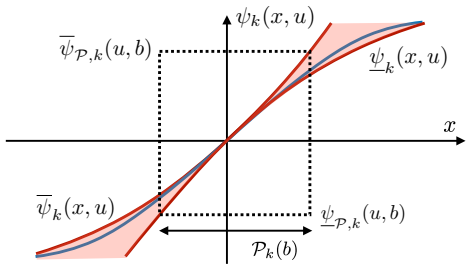

Fig. 2. Illustration of the concave envelope (in red) for the function $\psi(x,u)$ (in blue) and the corresponding bounds on $\psi(x,u)$ over the interval $\mathcal{P}_k(b)$.

Theorem 2. (Convex Restriction of Power Flow Feasibility Constraints) Given the operating point $u = (p_{\text{pv}},\ v_{\text{g}})$, there

exists a solution for the state $x = (\theta_{\text{ns}}, v_{\text{pq}})$ that satisfies the AC OPF constraints (2), (3) if there exist $b = (\overline{\varphi},\, \overline{v}_{\text{pq}},\, -\underline{\varphi},\, -\underline{v}_{\text{pq}})$ and $(\overline{s}^{\text{f}}, \overline{s}^{\text{t}})$ such that

$$-AJ_{f,0}^{-1}\tau(u) + K^{+}\overline{g}_{\mathcal{P}}(u,b) + K^{-}\underline{g}_{\mathcal{P}}(u,b) \le b, \tag{18}$$

$$\begin{aligned}
M_{\text{ineq}}^{+}\overline{\psi}_{\mathcal{P}}(u,b) + M_{\text{ineq}}^{-}\underline{\psi}_{\mathcal{P}}(u,b) &\le \zeta(p_g^{\max}, q_g^{\max}),\\
M_{\text{ineq}}^{-}\overline{\psi}_{\mathcal{P}}(u,b) + M_{\text{ineq}}^{+}\underline{\psi}_{\mathcal{P}}(u,b) &\ge \zeta(p_g^{\min}, q_g^{\min}),\\
b \le b^{\max},\, u^{\min} \le u &\le u^{\max},\\
L_{\text{line}}^{\text{k},+}\overline{\psi}_{\mathcal{P}}(u,b) + L_{\text{line}}^{\text{k},-}\underline{\psi}_{\mathcal{P}}(u,b) &\le \overline{s}^{\text{k}}, \quad \text{k} \in \{\text{f},\text{t}\},\\
-L_{\text{line}}^{\text{k},-}\overline{\psi}_{\mathcal{P}}(u,b) - L_{\text{line}}^{\text{k},+}\underline{\psi}_{\mathcal{P}}(u,b) &\le \overline{s}^{\text{k}}, \quad \text{k} \in \{\text{f},\text{t}\},\\
\left(\overline{s}_p^{\text{k}}\right)^2 + \left(\overline{s}_q^{\text{k}}\right)^2 &\le \left(s^{\max}\right)^2, \quad \text{k} \in \{\text{f},\text{t}\},
\end{aligned} \tag{19}$$

where $K = -AJ_{f,0}^{-1}M_{\text{eq}}$, and $\Lambda_{ij}^{+} = \max\{\Lambda_{ij}, 0\}$ and $\Lambda_{ij}^{-} = \min\{\Lambda_{ij}, 0\}$ for an arbitrary matrix Λ.

Proof. Condition (18) is sufficient to satisfy condition (15) in Brouwer's Fixed Point Theorem:

$$\begin{aligned}
&\max_{x\in\mathcal{P}(b)} Kg(x,u) - AJ_{f,0}^{-1}\tau(u)\\
&\qquad \le K^{+}\overline{g}_{\mathcal{P}}(u,b) + K^{-}\underline{g}_{\mathcal{P}}(u,b) - AJ_{f,0}^{-1}\tau(u) \le b.
\end{aligned}$$

Then for all $x \in \mathcal{P}(b)$, $-J_{f,0}^{-1}M_{\text{eq}}g(x,u) \in \mathcal{P}(b)$. By applying Brouwer's Fixed Point Theorem to (11), there exists a solution $x \in \mathcal{P}(b)$. Further, (19) ensures the operational constraints are satisfied for all $x \in \mathcal{P}(b)$. A more detailed proof is in [17]. □

Note the convex restriction can be written analytically using only the inversion of Jacobian at the base operating point.

B. Optimal Power Flow with Quadratic Convex Restriction

We obtain a conservative convex approximation of the AC OPF problem's feasible space by replacing the original AC OPF constraints (2), (3) with the convex restriction (18), (19). The objective function requires further consideration.

1) Objective Function: The objective is a function of the active power output from each generator ($p_{g,i}$). Since the active power generation at the slack (Vθ) bus is an implicit state variable, it is replaced by its over-estimator. Since the objective function is monotonically increasing with respect to the active power generation, the objective can be over-estimated by

$$\overline{c}(u,b) = c_{\text{v}\theta}(\overline{p}_{\text{g,v}\theta}) + \sum_{i=1}^{n_{\text{pv}}} c_{\text{pv},i}(p_{\text{pv},i}) \tag{20}$$

where $\overline{p}_{\text{g,v}\theta}$ is an over-estimator on the active power generated at the slack bus. This over-estimator is constrained by

$$C_{\text{v}\theta}\,\overline{p}_{\text{g,v}\theta} - p_{\text{d,v}\theta} \ge M_{\text{v}\theta}^{+}\,\overline{\psi}_{\mathcal{P}}(u,b) + M_{\text{v}\theta}^{-}\,\underline{\psi}_{\mathcal{P}}(u,b), \tag{21}$$

where $M_{\text{v}\theta} \in \mathbb{R}^{1\times(2n_l+n_b)}$ is the row of M_{ineq} that corresponds to the active power generation limit at the Vθ bus.

2) OPF with Convex Restriction: The AC OPF is given by

$$\begin{array}{lll}
\underset{u,b,\overline{s}^{\text{f}},\overline{s}^{\text{t}},\overline{p}_{\text{g,v}\theta}}{\text{minimize}} & (20) & \text{objective function}\\
\text{subject to} & (18),(19),(21) & \text{convex restriction}
\end{array}$$

Remark 1. The solution for OPF with convex restriction ($p_{\text{g}}^{\text{cvxrs}}$) is lower bounded by the globally optimal solution of the original AC OPF problem (p_{g}^{*}) and is upper bounded by the objective value at the base point ($p_{\text{g},0}$):

$$c(p_{\text{g}}^{*}) \le c(p_{\text{g}}^{\text{cvxrs}}) \le c(p_{\text{g},0}).$$

Remark 2. The OPF with convex restriction (i.e., (18)–(21)) is a convex quadratically constrained quadratic program (convex QCQP) that can be solved with commercial solvers such as Mosek, CPLEX, and Gurobi. The number of quadratic constraints is bounded by $30n_l + 4n_b + 4n_g$.

Remark 1 states that the solution of OPF with convex restriction has reduced or equal objective value relative to the base point. Remark 2 indicates that the size of the resulting convex optimization problem increases linearly with the system size.

IV. Feasible Path Optimal Power Flow

We present an iterative algorithm to solve OPF with the convex restriction, while guaranteeing the existence of a feasible path to the new operating point.

A. Definition of the Feasible Path

The motivation for studying the feasible path is to bring the system from the current operating point to the desired operating point while guaranteeing steady-state stability, i.e., a trajectory which satisfies the AC power flow equations as well as the operational constraints. This leads to the following definition of a feasible path.

Definition 1. A *feasible path* between two control set points $u^{(0)}$ and $u^{(N)}$ is a set of control variables that forms a continuous trajectory connecting the two set points such that there exists state variables x that satisfy the AC OPF constraints in (2), (3) at every point along the trajectory.

In particular, the feasible path will be described by a sequence of control actions $u^{(k)}, i = 0,\ldots,N$ where

$$\mathcal{U} = \{\alpha u^{(k)} + (1-\alpha)u^{(k+1)} \mid \alpha \in [0,1],\ \forall k = 0,\ldots,N-1\}.$$

B. Feasible Path Identification Algorithm

The convex restriction provides an *inner approximation* of the power flow feasibility set that is a convex set. By the definition of a convex set, all points on the line connecting two operating points $u^{(k)}$ and $u^{(k+1)}$ within the convex restriction are guaranteed to be feasible. That is, for $\alpha \in [0,1]$,

$$\alpha u^{(k)} + (1-\alpha)u^{(k+1)} \in \mathcal{U}_{(k)}^{\text{cvxrstr}}. \tag{22}$$

Here, $\mathcal{U}_{(k)}^{\text{cvxrstr}}$ denotes the convex restriction (18), (19), constructed with the base point at $u^{(k)}$. By leveraging this property of convexity, we propose to use *sequential convex restrictions* to identify a feasible path. The algorithm based on Sequential Convex Restrictions is described in Algorithm 1. Given a current set of control variables $u^{(k)}$, each iteration of the algorithm (i) solves the power flow equations to obtain the base point $(x^{(k)}, u^{(k)})$, (ii) constructs the convex restriction at this

base point, and (iii) solves a convex restriction OPF to obtain a new set of control variables $u^{(k+1)}$. The output of the algorithm is a sequence of control set points $u^{(k)}, k = 0, \ldots, N$, that forms a piece-wise linear feasible path between the initial operating point $u^{(0)}$ and $u^{(N)}$.

Algorithm 1 Feasible Path Identification Algorithm with Sequential Convex Restriction

1: *Initialize*: Set $u^{(0)}$ and $x^{(0)}$ to the initial operating point.
2: **while** $\|u^{(k+1)} - u^{(k)}\|_2 > \varepsilon$ **do**
3: Solve power flow given $u^{(k)}$ to obtain $x^{(k)}$.
4: Set $x_0 = x^{(k)}$ and compute the power flow Jacobian at the base point ($J_{f,0}$).
5: Construct Convex Restriction ($\mathcal{U}_{(k)}^{\text{cvxrstr}}$) with (18), (19).
6: Solve
$$u^{(k+1)} = \underset{u \in \mathcal{U}_{(k)}^{\text{cvxrstr}}}{\arg\min}\, f_0(u, b). \tag{23}$$
7: $k := k + 1$.
8: **end while**
9: **return** $u^{(1)}, \ldots, u^{(N)}$.

A related type of algorithm is Sequential Convex Programming, which relies on the approximation of the equations over a trust region in order to solve an optimization problem [19], [20]. Unlike general Sequential Convex Programming, our algorithm based on Sequential Convex Restriction ensures feasibility at every point along the associated path.

C. Operational Scenarios for Feasible Path OPF

Depending on the problem setting, we might want to consider different objective functions f_0 in (23). We provide two examples.

1) Optimal Power Flow with Feasible Path Guarantees: Given the current, sub-optimal operating point (x_0, u_0), we want to find a lower cost operating point (x^*, u^*) while guaranteeing a feasible path between the two points. In this formulation, the OPF problem is directly solved by setting the objective to be the cost of generation:

$$f_0(u, b) = \bar{c}(u, b), \tag{24}$$

where $\bar{c}(u, b)$ is defined in (20).

2) Feasible Path Identification for Known Operating Points: In an alternative scenario, we are provided a known, desired operating point $(p_{\text{pv}}^*, v_{\text{g}}^*)$ and seek a sequence of feasible control actions which bring the system towards the desired point. The objective function here minimizes the Euclidean distance from the desired generation set point

$$f_0(u, b) = \lambda \|p_{\text{pv}} - p_{\text{pv}}^*\|_2 + \|v_{\text{g}} - v_{\text{g}}^*\|_2 \tag{25}$$

where λ is a relative weighting of the differences in generator power injections and voltage magnitudes. The convergence of the algorithm depends on the weight λ, which will be investigated further in the numerical studies section.

D. Convergence of the Feasible Path OPF

The sequential convex restriction may not always converge to the optimal solution. We provide a few scenarios in which the algorithm may not arrive at the desired operating point.

- If the initial and the optimal operating points belong to separate, disconnected regions of the feasible space, there is no feasible path between the two points. The algorithm's final point will reside in the region with the initial point.
- The algorithm could converge to a point at the nonconvex boundary of the feasible set where all cost-descending directions are infeasible.

The next section provides quantitative experiments to show the convergence of the algorithm on standard IEEE test cases.

V. Numerical Studies

This section computationally demonstrates our algorithm. Two illustrative examples are presented to visualize how the algorithm finds a feasible path to a desired point and to study the convergence characteristics. Extensive numerical studies show how the algorithm improves the initial solution.

A. Implementation

The studies were conducted using the test cases from PGLib v19.01 [21] with sizes up to the 588 buses. Computations were done using a laptop with a 3.3 GHz Intel Core i7 processor and 16 GB of RAM. The code implementation uses JuMP/Julia [22]. MOSEK was used to solve the convex QCQPs associated with the convex restrictions. MATPOWER's interior point method was used to solve the AC OPF problems to obtain desired operating points [23]. Algorithm 1 was implemented with $\varepsilon = 0.01$, where the power flow in each iteration (step 3) was solved using the Newton-Raphson method.

B. Illustrative Example: Finding a Feasible Path

We first show an illustrative example of a feasible path identified for the 9-bus system [24]. In this experiment, the voltage magnitudes at the generators were fixed at 1 p.u . and the generators' reactive power limits were reduced from 300 MVAr to 100 MVAr. Fig. 3 shows the changes in the control variable set points as the algorithm progresses. The algorithm converges to the desired operating point in 7 iterations. The figure shows that the piece-wise linear path goes around the infeasible operating region (plotted in white) and arrives at the desired operating point without violating any OPF constraints.

C. Convergence of Feasible Path Identification for Known Operating Point

In this study, we investigate convergence of the feasible path algorithm in an example based on the IEEE 39-bus system [25]. The desired operating point was set to the globally optimal AC OPF solution. The initial operating point was determined by solving OPF with linear uniform generation cost (i.e., $c(p_g) = \sum_i p_{g,i}$) using MATPOWER. The distance between the current and the desired operating point was minimized with different values of the parameter λ in the objective in (25), which determines the trade-off between convergence for the active power and voltage magnitudes.

Fig. 4 shows the convergence of the active power generation and voltage magnitudes to the desired operating point. For

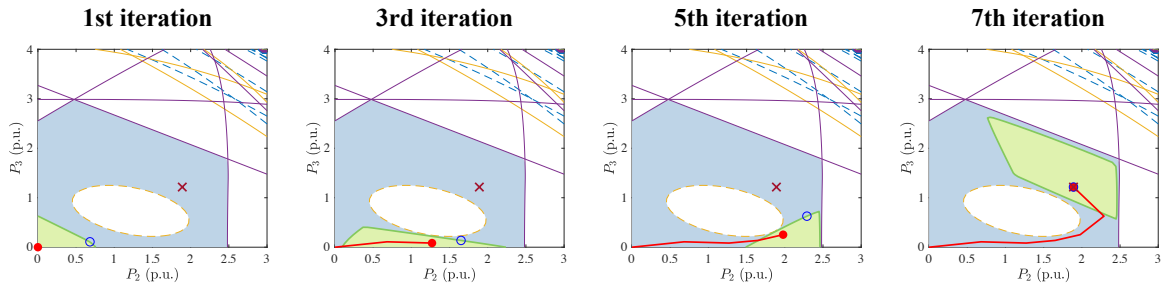

Fig. 3. Illustration of Sequential Convex Restriction in the 9-bus system for the first, third, fifth, and seventh iterations. The feasibility space is shown in blue and the convex restriction is shown in green. The optimal solution is marked by the $\times$ symbol and the red line shows the feasible path.

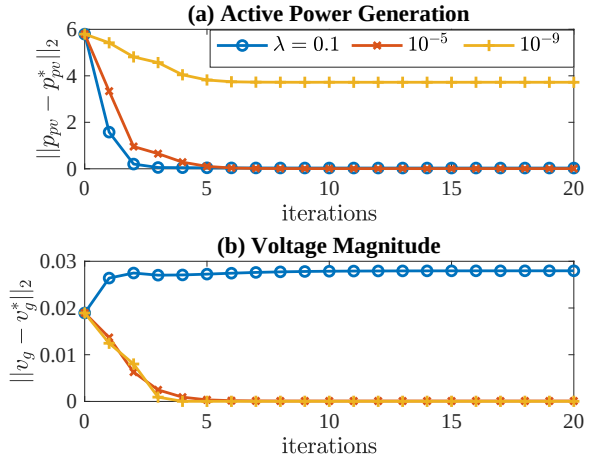

Fig. 4. Convergence of the feasible path to the identified point for varying values of λ for the 39-bus system.

large enough values of λ, the active power outputs (at the non-slack generators) converge to those of the desired operating point. However, the voltage magnitudes may converge to a different, sub-optimal power flow solution. Similarly, if λ is set too low, the voltage magnitudes may converge to the desired operating point, while the active power set points do not. For intermediate values of λ, both active power and voltage magnitudes converge to the desired point.

The main takeaway from this result is that the convergence of the algorithm is path-dependent, i.e., there are cases where the sequential convex restriction gets trapped in a sub-optimal point. This issue could be mitigated by appropriate tuning of the objective function.

D. Optimal Power Flow with Feasible Path Guarantees

To show how the algorithm improves an initial, sub-optimal point (using the objective function (24)), we run our algorithm on different PGLib test cases. The initial operating point was obtained by solving the OPF problem with a linear uniform generation cost ($\sum_i p_{g,i}$) in MATPOWER. These solutions are far from the optima of the OPF problems with their original (generation cost minimizing) objective functions. Thus, this experimental setup adequately exercises our Sequential Convex Restriction algorithm.

Table I summarizes the numerical studies where the cost of generation was minimized at each iteration of the algorithm. The costs after the first and last iteration of the sequential convex restriction are shown in the fourth and fifth columns of Table I. The optimality gap at the ith iteration is defined as

$$\text{Optimality Gap} = \frac{c(p_g^{(i)}) - c(p_g^*)}{c(p_g^*)}. \tag{26}$$

Here, $c(p_g)$ is the objective function (10a), $p_g^{(i)}$ is the power generation at the ith iteration and p_g^* is the optimal set point from MATPOWER. We observe that the OPF with convex restriction is able to significantly improve the operating point from the initial point, even if it does not reach the same solution as MATPOWER. The algorithm converges within 5 iterations for all cases. The average solver time per iteration is also shown in the last two columns. Note that the algorithm is also applicable to larger systems.

Note that the Sequential Convex Restriction algorithm encountered numerical problems for two test cases (the 89- and 240-bus systems), which are omitted from the results in Table I. The source of these problems is the line flow limits, which add quadratic limits on the existing quadratic envelopes. Essentially, this introduces higher-order polynomial constraints (expressed in terms of two quadratic constraints), which can cause numerical problems.

VI. Conclusion

This paper proposes an Sequential Convex Restriction algorithm to obtain a *feasible path* from an initial, feasible operating point to an improved operating point. The feasible path is a trajectory for which all points are AC power flow feasible and satisfy all operational constraints. The algorithm relies on solving a sequence of OPF problems that are formulated using so-called convex restrictions, which are conservative, convex inner approximations of the OPF feasible space. The case studies demonstrate that the sequential convex restriction algorithm converges to a high-quality solution while generating feasible control actions, and is scalable to large systems.

Extensions of the work proposed in this paper include the consideration of dynamic stability and applying related convex restriction techniques to guarantee robustly feasible solutions to AC OPF problems.

Appendix

Let $E_f \in \mathbb{R}^{n_b \times n_l}$ and $E_t \in \mathbb{R}^{n_b \times n_l}$ be the connection matrix for *from* and *to* buses. The $(k,l)^{\text{th}}$ element of E_f and

TABLE I
OPTIMALITY GAPS AND RUNTIMES OF OPF WITH CONVEX RESTRICTION FOR SELECTED PGLIB TEST CASES

Test Case	Objective ($/h)				Number of iterations	Optimality Gap (%)		Solver Time (seconds)
	Initial	MATPOWER	CVXRS 1st iter	CVXRS last iter		1st iter	last iter	
pglib_opf_case3_lmbd	6089.54	5812.64	5986.53	5813.54	5	2.99	0.02	0.01
pglib_opf_case5_pjm	27356.2	17551.9	17839	17578.8	4	1.64	0.15	0.03
pglib_opf_case14_ieee	7008.23	6291.28	6291.35	6291.29	2	0	0	0.08
pglib_opf_case24_ieee_rts	87065.8	63352.2	63393.8	63361.5	4	0.07	0.01	0.19
pglib_opf_case30_ieee	12308.3	11974.5	11981.1	11976.8	2	0.06	0.02	0.23
pglib_opf_case39_epri	152592	142980	144525	143010	4	1.08	0.02	0.41
pglib_opf_case57_ieee	46216.5	39323.4	44000.3	42494	5	11.89	8.06	1.04
pglib_opf_case73_ieee_rts	262108	189764	189908	189789	5	0.08	0.01	1.73
pglib_opf_case118_ieee	145657	115804	117068	116071	5	1.09	0.23	3.55
pglib_opf_case162_ieee_dtc	129083	126154	127622	127612	3	1.16	1.16	19.91
pglib_opf_case179_goc	905329	828404	893016	883301	5	7.8	6.63	11.47
pglib_opf_case200_tamu	37398.7	34730.7	37138.3	35895.9	5	6.93	3.35	10.21
pglib_opf_case300_ieee	850620	664220	734711	684909	5	10.61	3.11	55
pglib_opf_case588_sdet	476950	381555	447566	428569	5	17.3	12.32	219.66

the $(m,l)^{\text{th}}$ element of E_t are equal to 1 for each transmission line l, where the line l connects the "from" bus k to "to" bus m, and zero otherwise, and $E = E_f - E_t$. The matrices Y_{ff}, Y_{tf}, Y_{ft} and Y_{tt} are diagonal with its elements,

$$Y_{\text{ff},kk} = \left(y_k + j\frac{b_k^c}{2}\right)\left(\frac{1}{\tau_k}\right)^2, \quad Y_{\text{tt},kk} = y_k + j\frac{b_k^c}{2},$$
$$Y_{\text{ft},kk} = -y_k\frac{1}{\tau_k e^{-j\theta_k^{\text{shift}}}}, \qquad Y_{\text{tf},kk} = -y_k\frac{1}{\tau_k e^{j\theta_k^{\text{shift}}}}.$$

where $Y_{\text{ff},kk}$ represents k^{th} row and k^{th} column of the diagonal matrix Y_{ff}. The transformer tap ratio, phase shift angle, and line charging susceptance are τ, θ^{shift}, b^c, respectively. The phase adjusted admittance matrices $\widehat{Y}_{\text{ft}} \in \mathbb{C}^{n_l \times n_l}$ and $\widehat{Y}_{\text{tf}} \in \mathbb{C}^{n_l \times n_l}$ are diagonal matrices with

$$\widehat{Y}_{\text{ft}} = Y_{\text{ft}}\mathbf{diag}\left(e^{-j\varphi_0}\right), \quad \widehat{Y}_{\text{tf}} = Y_{\text{tf}}\mathbf{diag}\left(e^{j\varphi_0}\right).$$

where each diagonal element of $\widehat{Y}_{\text{ft}}$ is an adjustment of Y_{ft} by angle φ_0. Then

$$\widehat{Y}^{\text{c}} = E_{\text{f}}\widehat{Y}_{\text{ft}} + E_{\text{t}}\widehat{Y}_{\text{tf}}, \quad \widehat{Y}^{\text{s}} = E_{\text{f}}\widehat{Y}_{\text{ft}} - E_{\text{t}}\widehat{Y}_{\text{tf}},$$
$$Y^{\text{d}} = E_{\text{f}}Y_{\text{ff}}E_{\text{f}}^T + E_{\text{t}}Y_{\text{tt}}E_{\text{t}}^T + Y_{\text{sh}}.$$

Replacing Y by G or B yields the real and imaginary parts of the Y matrix, which are used in (5), (8), and (9).

REFERENCES

[1] B. Stott and O. Alsaç, "Optimal Power Flow–Basic Requirements for Real-Life Problems and their Solutions," in *12th Symp. Specialists in Electric Operational and Expansion Planning (SEPOPE)*, May 2012.

[2] J. Carpentier, "Contribution a l'Etude du Dispatching Economique," *Bull. Soc. Franc. des Electriciens*, vol. 8, no. 3, pp. 431–447, 1962.

[3] S. H. Low, "Convex Relaxation of Optimal Power Flow–Part I: Formulations and Equivalence," *IEEE Trans. Control Network Syst.*, vol. 1, no. 1, pp. 15–27, March 2014.

[4] C. Coffrin, H. L. Hijazi, and P. Van Hentenryck, "The QC Relaxation: A Theoretical and Computational Study on Optimal Power Flow," *IEEE Trans. Power Syst.*, vol. 31, no. 4, pp. 3008–3018, July 2016.

[5] A. J. Wood and B. F. Wollenberg, *Power Generation, Operation, and Control*. J. Wiley & Sons, 1996.

[6] D. K. Molzahn and I. A. Hiskens, "A Survey of Relaxations and Approximations of the Power Flow Equations," *Found. Trends Electric Energy Syst.*, vol. 4, no. 1-2, pp. 1–221, Feb. 2019.

[7] F. Capitanescu *et al.*, "State-of-the-Art, Challenges, and Future Trends in Security Constrained Optimal Power Flow," *Electric Power Syst. Res.*, vol. 81, no. 8, pp. 1731 – 1741, 2011.

[8] T.-G. L. Y.-Y. Hong, C.-M. Liao, "Application of Newton Optimal Power Flow to Assessment of VAR Control Sequences on Voltage Security: Case Studies for a Practical Power System," *IEE Proc. C (Generation, Transmission and Distribution)*, vol. 140, pp. 539–544, Nov 1993.

[9] F. Capitanescu and L. Wehenkel, "Redispatching Active and Reactive Powers using a Limited Number of Control Actions," *IEEE Trans. Power Syst.*, vol. 26, no. 3, pp. 1221–1230, Aug. 2011.

[10] D. T. Phan and X. A. Sun, "Minimal Impact Corrective Actions in Security-Constrained Optimal Power Flow via Sparsity Regularization," *IEEE Trans. Power Syst.*, vol. 30, no. 4, pp. 1947–1956, 2014.

[11] W. A. Bukhsh, A. Grothey, K. I. M. McKinnon, and P. A. Trodden, "Local Solutions of the Optimal Power Flow Problem," *IEEE Trans. Power Syst.*, vol. 28, no. 4, pp. 4780–4788, 2013.

[12] A. Bernstein, L. Reyes-Chamorro, J.-Y. Le Boudec, and M. Paolone, "A Composable Method for Real-Time Control of Active Distribution Networks with Explicit Power Setpoints. Part I: Framework," *Electric Power Syst. Res.*, vol. 125, pp. 254–264, Aug. 2015.

[13] C. Wang, J.-Y. Le Boudec, and M. Paolone, "Controlling the Electrical State via Uncertain Power Injections in Three-Phase Distribution Networks," *IEEE Trans. Smart Grid*, pp. 1–1, 2017.

[14] A. Lorca and X. A. Sun, "The Adaptive Robust Multi-Period Alternating Current Optimal Power Flow Problem," *IEEE Trans. Power Syst.*, vol. 33, no. 2, pp. 1993–2003, 2017.

[15] R. Louca and E. Bitar, "Robust AC Optimal Power Flow," *arXiv:1706.09019*, June 2017.

[16] D. K. Molzahn and L. A. Roald, "Towards an AC Optimal Power Flow Algorithm with Robust Feasibility Guarantees," in *20th Power Syst. Computat. Conf. (PSCC)*, June 2018.

[17] D. Lee, H. D. Nguyen, K. Dvijotham, and K. Turitsyn, "Convex restriction of power flow feasibility sets," *arXiv:1803.00818*, 2018.

[18] L. E. J. Brouwer, "Über abbildung von mannigfaltigkeiten," *Mathematische Annalen*, vol. 71, no. 1, pp. 97–115, 1911.

[19] A. R. Conn, N. I. M. Gould, and P. L. Toint, *Trust Region Methods*. SIAM, 2000, vol. 1.

[20] J. Nocedal and S. Wright, *Numerical Optimization*. Springer Science & Business Media, 2006.

[21] IEEE PES Task Force on Benchmarks for Validation of Emerging Power System Algorithms, "Power Grid Lib – Optimal Power Flow," https://github.com/power-grid-lib/pglib-opf.

[22] I. Dunning, J. Huchette, and M. Lubin, "JuMP: A Modeling Language for Mathematical Optimization," *SIAM Rev.*, vol. 59, no. 2, 2017.

[23] R. D. Zimmerman, C. E. Murillo-Sánchez, and R. J. Thomas, "MATPOWER: Steady-State Operations, Planning, and Analysis Tools for Power Systems Research and Education," *IEEE Trans. Power Syst.*, vol. 26, no. 1, pp. 12–19, 2011.

[24] J. H. Chow, G. Peponides, P. V. Kokotovic, B. Avramovic, and J. R. Winkelman, *Time-Scale Modeling of Dynamic Networks with Applications to Power Systems*. Springer, 1982, vol. 46.

[25] M. A. Pai, *Energy Function Analysis for Power System Stability*. Springer Science & Business Media, 2012.